Pyramid shape of polymer solar cells: a simple solution to triple efficiency

Pyramid shape of polymer solar cells: a simple solution to triple efficiency

OPEN ACCESS
IOP PUBLISHING JOURNAL OF PHYSICS D: APPLIED PHYSICS
J. Phys. D: Appl. Phys. **46** (2013) 305101 (6pp) doi:10.1088/0022-3727/46/30/305101

Pyramid shape of polymer solar cells: a simple solution to triple efficiency

Yuxin Xia[1], Lintao Hou[1,4], Kaijie Ma[1], Biao Wang[1], Kang Xiong[1], Pengyi Liu[1], Jihai Liao[2], Shangsheng Wen[2,4] and Ergang Wang[3]

[1] Siyuan Laboratory, Department of Physics, Jinan University, Guangzhou 510632, People's Republic of China
[2] State Key Laboratory of Luminescent Materials and Devices, South China University of Technology, Guangzhou 510640, People's Republic of China
[3] Department of Chemical and Biological Engineering/Polymer Technology, Chalmers University of Technology, SE-412 96 Göteborg, Sweden

E-mail: thlt@jnu.edu.cn (L T Hou) and shshwen@scut.edu.cn (S S Wen)

Received 24 January 2013, in final form 9 April 2013
Published 2 July 2013
Online at stacks.iop.org/JPhysD/46/305101

Abstract
Pyramid-shaped polymer solar cells fabricated on flexible substrates were investigated. Effective light trapping can be realized due to light reflection in all 360° directions, and 100% space utilization is achieved when assembled into arrays. The power conversion efficiency is enhanced by 200% ([60]PCBM as the acceptor) and 260% ([70]PCBM as the acceptor) with a dihedral angle of 30° between the opposite sides of the pyramid compared with a planar device, and a high V_{oc} of 3.5 V in series connection is obtained. Considering the material utilization, an angle of 90° for pyramid-shaped polymer solar cells is proposed. Pyramid-shaped polymer solar cells are particularly suitable for installation on roof of vehicles and houses, which have limited surface area.

(Some figures may appear in colour only in the online journal)

1. Introduction

Polymer solar cells (PSCs) have shown their advantages in producing flexible and photovoltaic modules using printing methods at a low cost [1–3]. Nowadays, most efforts on improving power conversion efficiency (PCE) of PSCs have been focused on designing new low band gap materials [4, 5], adopting tandem structures and optimizing film microstructures [6–10], etc. As a result, single active layer PSCs based on conjugated polymers and fullerene bulk heterojunctions (BHJs) have reached a PCE of 8–9% [11, 12], approaching the 10% requirement for commercialization. However, further improvement of PCE of the flat device with a single active layer by the above-mentioned methods seems not so easy as the PCE approaches its theoretical upper limit [13, 14]. On the other hand, a simple solution to improve PCE using geometrical device structures receives only limited attention. V-shaped and multifold PSCs that can absorb reflected photons from the adjacent cell were demonstrated by Inganäs and co-workers [15, 16] and cone-shaped PSCs, which can achieve effective light trapping due to multi-absorption in all 360° directions, were studied by Zhen *et al* [17]. By inducing a non-planar or three-dimensional geometrical device structure, a PCE could be enhanced obviously by harvesting more photons. V-shaped and cone-shaped PSCs both get PCE enhanced through more efficient light trapping and redistribution. Yet, V-shaped devices cannot trap light in all 360° directions, though they have advantages when assembled into device arrays. Cone-shaped devices are not suitable to be assembled into device arrays, for there are vacant spaces between adjacent devices as they have circle bases serving as the plane of light incidence. Moreover, cone-shaped devices can only be made on flexible plastic substrates. Here we demonstrate pyramid-shaped PSCs with light trapping in all 360° directions as well as 100% space utilization when assembled into device arrays, as demonstrated in figures 1(*a*)–(*c*). The advantage of pyramid-shaped PSCs is that they can make full use of a limited area such as the roof of a house or motor vehicles. As shown in this work, triple

[4] Authors to whom any correspondence should be addressed.

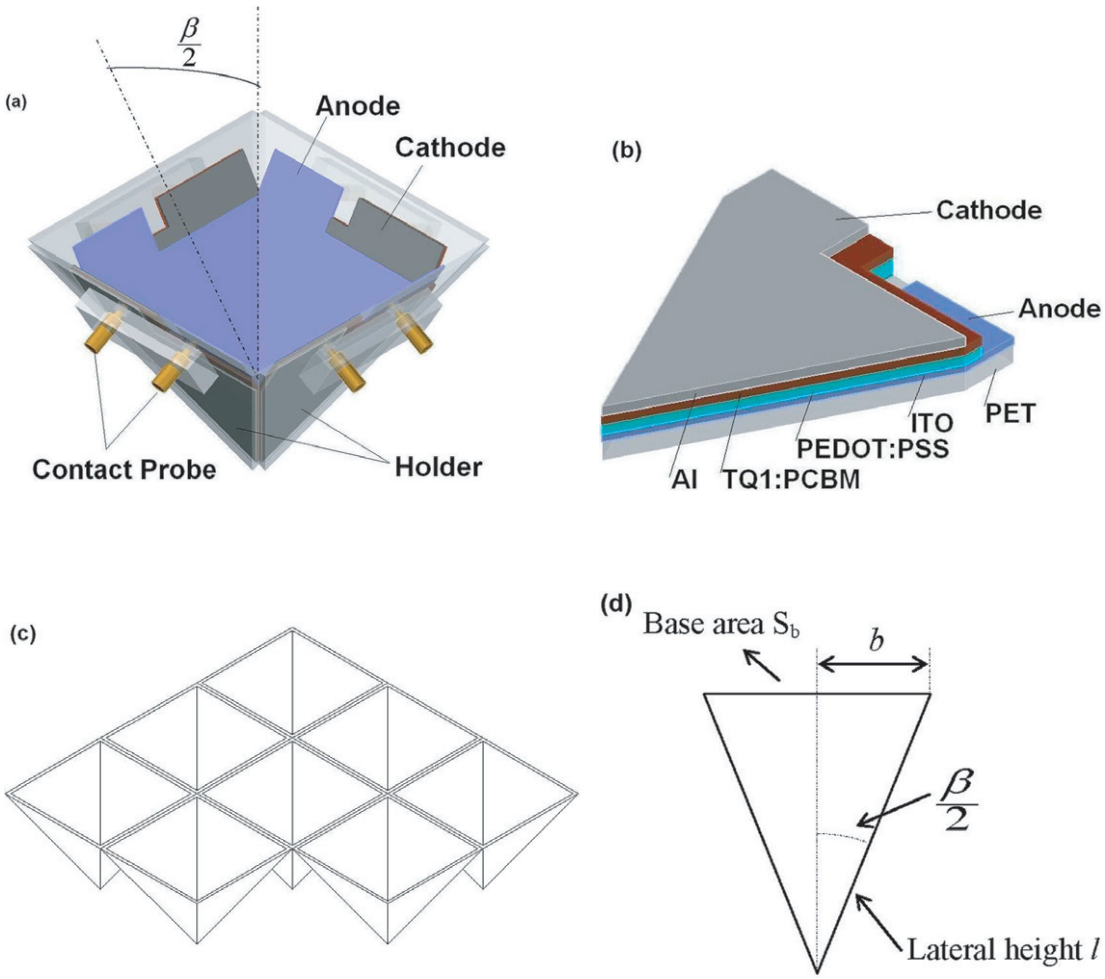

Figure 1. (*a*) Sketch of a pyramid-shaped device. Four triangle solar cells served as the lateral sides of the pyramid-shaped device. The angle of two opposite sides of the pyramid is defined as β. (*b*) The structure of the solar cells; a typical structure is Al/TQ1 : PCBM/PEDOT : PSS/ITO on the PET substrate. (*c*) Pyramid devices achieve 100% surface occupation when assembled into an array. (*d*) Geometric parameters of the cross-section of the pyramid device.

efficiency was realized by pyramid-shaped PSCs compared with the planar one.

2. Device design and experiment

To simplify the preparation of pyramid-shaped PSCs, they were made on ITO-coated flexible plastic substrates. The sketch and geometric parameters of the pyramid-shaped device are depicted in figure 1. The pyramid-shaped device was composed of four independent triangular solar cells with a fixed device area of 1 cm^2 for each. The four solar cells were placed on a particular pyramid-shaped holder to serve as the four lateral sides of the pyramid, so that the lateral area of the pyramid-shaped device was 4 cm^2 in total. There were eight copper contact probes mounted on the holder, two for each cell, which can make tight contact to the electrodes of the solar cells. With these probes, the cells could be connected in series, parallel and series–parallel to produce an appropriate open-circuit voltage (V_{oc}) and short-circuit current density (J_{sc}). We defined the dihedral angle between the two opposite lateral sides of the pyramid as β. For the pyramid-shaped devices with different β, we set the same lateral area as 4 cm^2.

Pyramid devices with β equal to 30°, 45°, 60° and 90° as well as planar devices (180°) were fabricated and tested. The single dependent triangle cells were fabricated on flexible ITO-coated polyethylene terephthalate (PET) plastic substrates with a typical BHJ structure ITO/PEDOT : PSS (PVP Al 4083)/poly[2, 3-bis-(3-octyloxyp-henyl) quinoxaline-5,8-diyl-*alt*-thiophene-2,5-diyl] (TQ1) : PCBM/Al. The thickness of the PET substrate was 0.13 mm with transmission >80% in a wide spectral range. The ITO sheet resistance was $45 \pm 5\ \Omega/\square$. Here we chose a high-performance low band gap polymer TQ1 blended with [60]PCBM or [70]PCBM as the active layer material [18]. The first step was to get the ITO-coated PET substrates ultrasonically cleaned with detergent, acetone, alcohol and de-ionized water followed by a UV/ozone treatment. As a buffer layer, the conductive polymer PEDOT : PSS (Baytron P VP Al 4083) (around 45 nm) was then spin-coated onto the ITO-coated PET substrates, followed by annealing at 65 °C for 1 h. The active layer of TQ1 : PCBM (around 90 nm) was spin-coated from a 1,2-dichlorobenzene (ODCB) solution. The TQ1 and [60]PCBM were blended by 1 : 2.5 (wt%), 40 mg ml^{-1} polymer content. The TQ1 and [70]PCBM were blended by 1 : 2.7 (wt%), 37 mg ml^{-1} polymer content. The thicknesses were determined by an

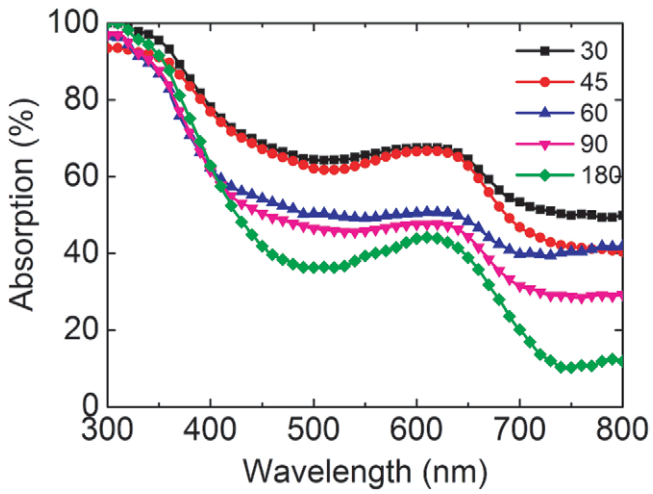

Figure 2. Absorption of the pyramid-shaped active layers (TQ1 : [60]PCBM) with β changing from 180° to 30°.

AMBIOS Technology XP-2 surface profiler. A 100 nm thick Al cathode was thermally deposited under high vacuum using a mask to define the active area of each cell. PCE was calculated from the J–V characteristic recorded by a Keithley 2400 source meter under illumination of an AM 1.5G solar simulator with an intensity of 100 mW cm^{-2} (Sun 2000 solar simulator, ABET technologies). The light intensity of the solar simulator was calibrated by a standard silicon photodiode. The incident photon-to-current conversion efficiency (IPCE) data were tested using a Crowntech-1000 IPCE test system from Crowntech, Inc.

3. Results and discussion

3.1. Absorption of the pyramid device

The absorption efficiency of the pyramid devices depends on the angle β. Figure 2 shows the absorption of the TQ1 : [60]PCBM films in the form of pyramid shape. The absorption throughout the whole visible range gets stronger as β decreases from 180° to 30°. This is because as β decreases, the light irradiated on the active layer per unit area could be more diluted and so the light could be absorbed more efficiently. Meanwhile, as β decreases, the incident light could probably be reflected more times which means more times of light absorption in the device, and this also helps the light trapping. So as β decreases, the light trapping effect is more efficient, leading to an enhancement of photon harvesting and J_{sc}.

3.2. Photovoltaic performance enhancement

Figures 3(*a*), (*b*) and (*c*) show the J–V curves of the pyramid-shaped devices with [60]PCBM as the acceptor in three ways of connections, respectively. Figures 4(*a*), (*b*) and (*c*) show the J–V curves for [70]PCBM devices. For [60]PCBM devices, V_{oc} is 3.18 V in series, 0.79 V in parallel and 1.56 V in series–parallel connections. It is observed that the value of V_{oc} in the same connection has no obvious change when β changes from 30°to 90°. In contrast, J_{sc} increases dramatically as β decreases, because devices with a smaller β can trap light more efficiently, as indicated in figure 2. The devices with the same β in different connections get similar PCEs though different V_{oc} and J_{sc}. Figure 3(*d*) shows the PCE enhancement rates of the pyramid device compared with the planar one (180°) along with the dihedral angle β. The enhancement rate increases with the decrease in β. For β equal to 30°, the PCE in series is significantly enhanced up to 200%. Even for 90°, an enhancement of 38% is achieved. Because the highest enhancement was achieved at $\beta = 30°$, devices with [70]PCBM as acceptor instead of [60]PCBM were also fabricated and tested with this angle. Since [70]PCBM exhibits better absorption than [60]PCBM, they presented a much better photovoltaic performance and so higher enhancement, up to 260%. The photovoltaic data of pyramid-shaped devices with different β under AM 1.5G are presented in tables 1 and 2. The PCEs reach 3.8–3.9% and 5.4–5.5% at an angle of 30° in three ways of connection compared with 1.3–1.4% and 1.5–1.6% at an angle of 180° for [60]PCBM devices and [70]PCBM devices, respectively. The enhancements of J_{sc} and PCE prove that the pyramid structure helps the photon harvesting. In addition, since no vacant spaces exist between pyramid-shaped devices when assembled into arrays, nearly 100% space utilization could be achieved, which is superior to the cone-shaped PSCs.

Four cells laid flat (180°) in three different connection ways achieve a similar photovoltaic performance. To understand the influence of illustration area on the photovoltaic performance of the devices, we also made planar solar cells with a much smaller active area of 0.05 cm^2. For the small-area cells, a PCE up to 3.5% ([60]PCBM) and 5.1% ([70]PCBM) is achieved with FF around 50% and a high V_{oc} of 0.88 V. Note that as an LiF layer was not used in this work, the PCE is slightly lower than that reported in the literature [18]. When the active area is enlarged up to 1 cm^2(1.7–1.9%) and 4 cm^2 (1.3–1.5%), the PCEs drop down because the high resistance induced from the sheet resistance of the films and the contact resistance results in lower FF and J_{sc} [19].

The IPCE of the pyramid devices (TQ1 : [60]PCBM) with different β was also measured under illumination of monochromatic light, as shown in figure 5. The IPCE curves correspond with the J–V curves: as β decreases, the devices can collect much more photon-induced carriers under the illumination of the monochromatic light covering the whole visible spectrum. Meanwhile the IPCE profiles are consistent with those of the corresponding absorption spectra, as shown in figure 2.

3.3. Material utilization

Although devices with a smaller β achieved higher PCE, the ratio of the base area S_b, also the illumination area of the device, to the lateral active area S_a becomes smaller. As demonstrated in figure 1(*d*), the base of the pyramid is a square with an area $S_b = (2 \times h)^2$, where h is the half side length of the square. The lateral area $S_a = 4 \times (l \times 2h/2)$, where l is the lateral

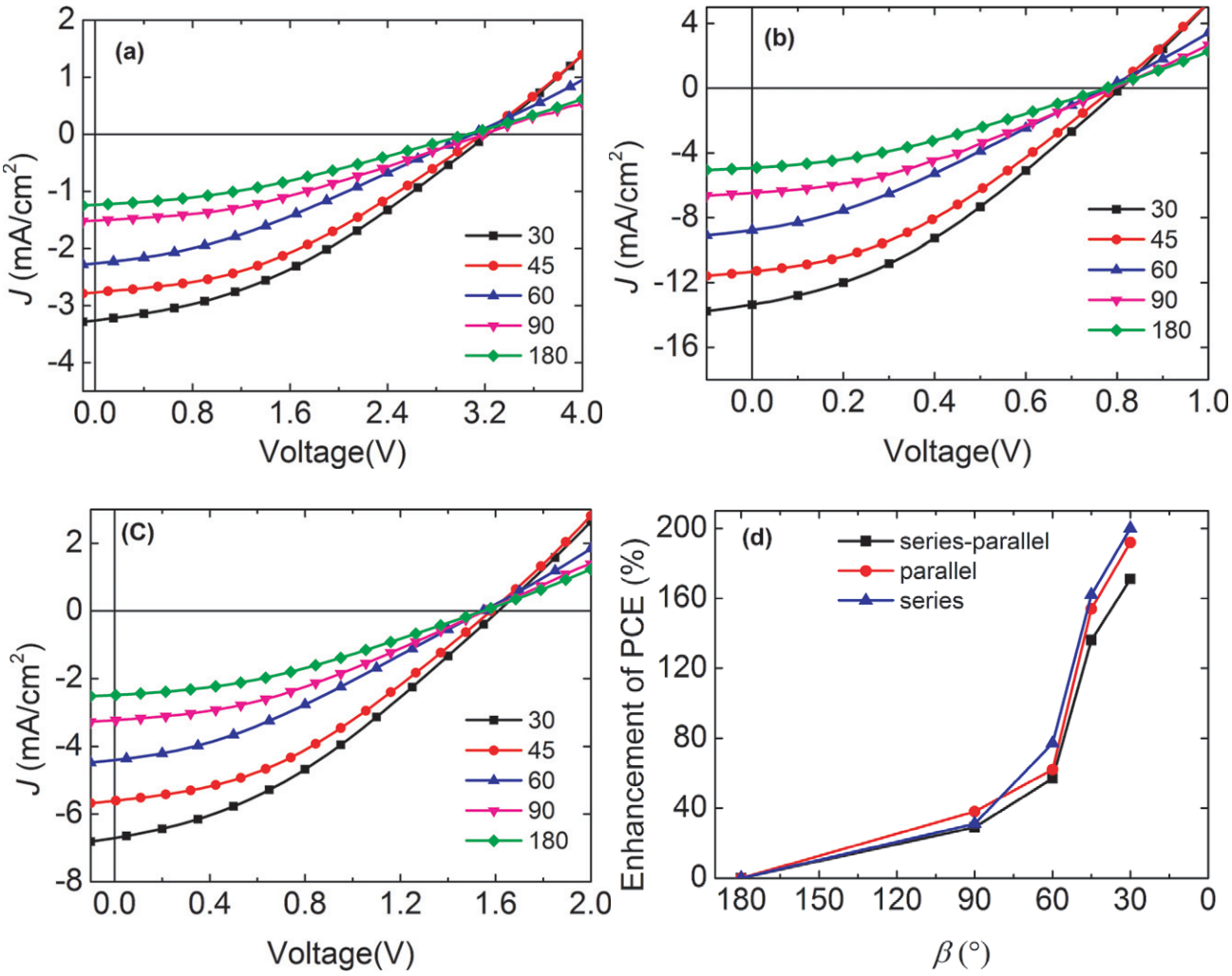

Figure 3. J–V characteristics of the pyramid devices using [60]PCBM as the acceptor (a) in series connection, (b) in parallel connection and (c) in series–parallel connection. (d) PCE enhancement rate of pyramid devices as a function of β.

height and equals $h/\sin(\beta/2)$. We take the ratio α as S_a/S_b to present the material utilization, so

$$\alpha = 4 \times h^2/(4 \times h^2/\sin(\beta/2)) = \sin(\beta/2).$$

Smaller α means more materials would be consumed to fabricate solar devices with a fixed illumination area. We also define another parameter $\gamma = \alpha \times \eta$, which presents the combination performance involving the material utilization and the PCE. It was found that γ for the device with $\beta = 90^\circ$ is the best and similar to that for the planar device with $\beta = 180^\circ$. However, the 90° pyramid device occupies a much smaller surface (2.83 cm^2) than the planar device (4 cm^2). For the pyramid device with $\beta = 30^\circ$, although it has the highest PCE, it gets the smallest γ (0.98). When the active area (S_a) of the pyramid device replaces the illumination area (S_b) in the calculation for $\beta = 90^\circ$, a PCE of 1.27% in parallel and series–parallel connections presents a similar light utilization to the planar one (1.3%).

3.4. Further discussion for industrial production

For large-scale industrial production, the inverted structure with a high PCE of more than 9% would be a preferred alternative for the solar cells and a much more efficient way can be introduced: first, the pyramid PET substrates can be produced using an injection modelling method, then all the functional layers including electrode layers, buffer layers and photovoltaic active layers along with interconnected lines among the four independent cells of the device can be made using a printing method on pyramid substrates. These devices would then be mounted on particular holders to constitute a large-area device array system.

4. Conclusions

In summary, we have presented a pyramid-shaped photovoltaic device using three ways of connections. The pyramid structure can not only realize 100% space utilization but also has higher light absorption efficiency due to the strong light trapping effect. The PCE for the 30° pyramid device was enhanced by 200% ([60]PCBM) and 260% ([70]PCBM), respectively, compared with the planar devices. This geometrical array is particularly suitable for installation on the roof of vehicles and houses, which have a limited surface area. A 90° pyramid device has more advantages when we consider the combination performance involving material utilization and PCE. A simple

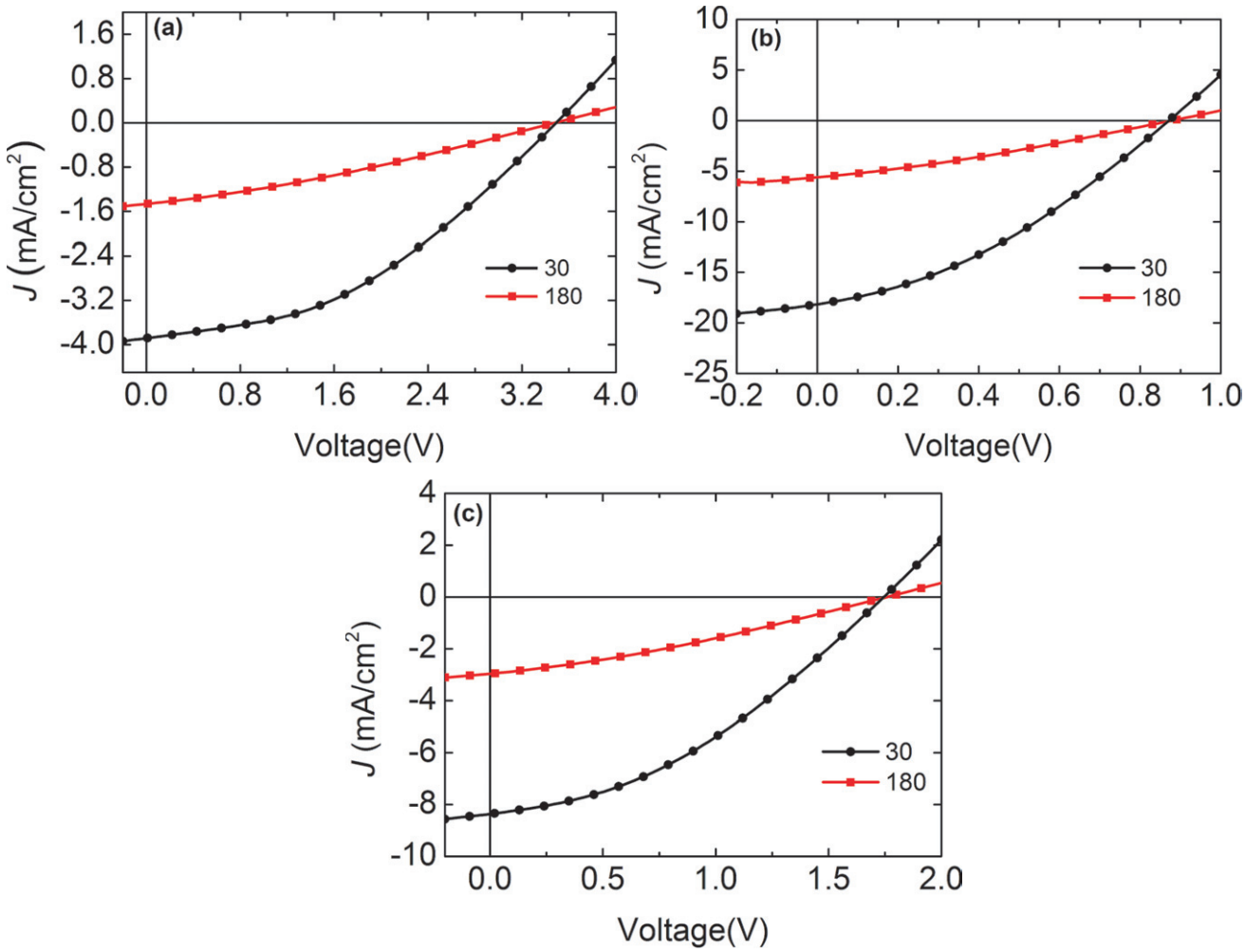

Figure 4. J–V characteristics of the pyramid devices at $\beta = 30^\circ$ and $\beta = 180^\circ$ using [70]PCBM as the acceptor (*a*) in series connection, (*b*) in parallel connection and (*c*) in series–parallel connection.

Table 1. Photovoltaic data of pyramid devices with different β using [60]PCBM as the acceptor under illumination of AM 1.5G. The values shown in the table are averaged values with standard deviation of devices of four batches made under identical conditions.

	β (°)	V_{oc} (V)	J_{sc} (mA cm^{-2})	FF (%)	η (%)
Series connection	30	3.25 ± 0.10	3.4 ± 0.2	36 ± 2	3.9 ± 0.1
	45	3.18 ± 0.09	2.8 ± 0.1	38 ± 1	3.4 ± 0.2
	60	3.10 ± 0.09	2.3 ± 0.2	32 ± 4	2.3 ± 0.1
	90	3.18 ± 0.11	1.5 ± 0.1	36 ± 2	1.7 ± 0.2
	180	3.10 ± 0.11	1.2 ± 0.2	34 ± 3	1.3 ± 0.1
Parallel connection	30	0.81 ± 0.01	13.4 ± 0.4	35 ± 2	3.8 ± 0.1
	45	0.79 ± 0.02	11.4 ± 0.3	36 ± 1	3.3 ± 0.2
	60	0.78 ± 0.03	8.8 ± 0.3	31 ± 3	2.1 ± 0.2
	90	0.79 ± 0.03	6.5 ± 0.2	36 ± 1	1.8 ± 0.1
	180	0.78 ± 0.03	4.9 ± 0.2	34 ± 3	1.3 ± 0.2
Series–parallel connection	30	1.61 ± 0.03	6.7 ± 0.1	35 ± 2	3.8 ± 0.1
	45	1.58 ± 0.04	5.6 ± 0.2	38 ± 1	3.3 ± 0.2
	60	1.55 ± 0.05	4.4 ± 0.2	32 ± 3	2.2 ± 0.2
	90	1.56 ± 0.03	3.2 ± 0.1	36 ± 2	1.8 ± 0.1
	180	1.55 ± 0.05	2.5 ± 0.2	35 ± 2	1.4 ± 0.2
Small planar cell	180	0.88 ± 0.01	7.8 ± 0.1	51 ± 1	3.5 ± 0.1

and feasible solution for improving PCE (up to 260%) of PSCs was demonstrated by the pyramid shape of PSCs in this work, which is anticipated to give a valuable method for the assembly of large-area PSC arrays.

Acknowledgments

The authors are grateful to the NSFC Project (#61274062 and #11204106) with the Open Fund of the State Key

Table 2. Photovoltaic data of pyramid devices with $\beta = 30^\circ$ using [70]PCBM as the acceptor under illumination of AM 1.5G. The values shown in the table are averaged values with standard deviation of devices of three batches made under identical conditions.

	β (°)	V_{oc} (V)	J_{sc} (mA cm^{-2})	FF (%)	η (%)
Series connection	30	3.50 ± 0.05	3.9 ± 0.1	40 ± 1	5.4 ± 0.2
	180	3.49 ± 0.03	1.5 ± 0.2	30 ± 3	1.5 ± 0.1
Parallel connection	30	0.87 ± 0.01	18.1 ± 0.4	36 ± 2	5.5 ± 0.2
	180	0.88 ± 0.01	5.6 ± 0.3	30 ± 1	1.5 ± 0.1
Series–parallel connection	30	1.74 ± 0.02	8.3 ± 0.2	37 ± 1	5.4 ± 0.2
	180	1.76 ± 0.02	3.0 ± 0.2	31 ± 2	1.6 ± 0.2
Small planar cell	180	0.88 ± 0.01	12.1 ± 0.1	48 ± 1	5.1 ± 0.1

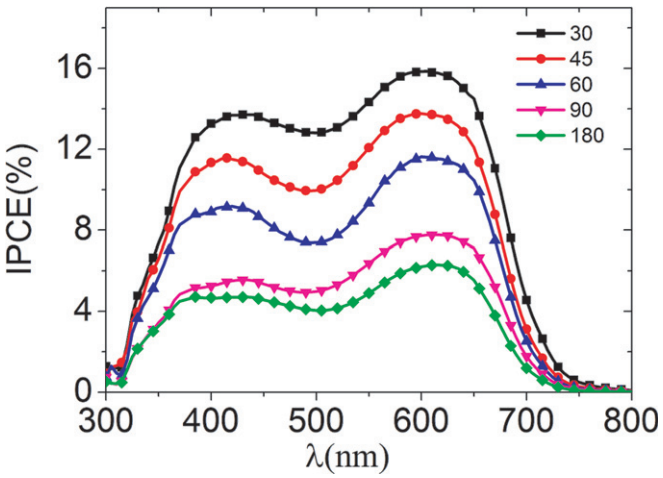

Figure 5. IPCE spectra of the pyramid-shaped devices using [60]PCBM as the acceptor with β changing from 180° to 30°.

Laboratory of Luminescent Materials and Devices (South China University of Technology#2012-skllmd-10) and the Science and Technology Planning Project of Guangdong Province (#2011A081301017, #2012A080304012 and #2012A08034001) for financial support. EW acknowledges the Swedish Research Council for financial support.

References

[1] Lungenschmied C, Dennler G, Neugebauer H, Sariciftci S N, Glatthaar M, Meyer T and Meyer A 2007 *Sol. Energy Mater. Sol. Cells* **91** 379
[2] Chen H Y, Hou J H, Zhang S Q, Liang Y Y, Yang G W, Yang Y, Yu L P, Wu Y and Li G 2009 *Nature Photon.* **3** 649
[3] Park S H, Roy A, Beaupre S, Cho S, Coates N, Moon J S, Moses D, Leclerc M, Lee K and Heeger A J 2009 *Nature Photon.* **3** 297
[4] Boudreault P L T, Najari A and Leclerc M 2011 *Chem. Mater.* **23** 456
[5] Price S C, Stuart A C, Yang L, Zhou H and You W 2011 *J. Am. Chem. Soc.* **133** 4625
[6] Niggemann M, Glatthaar M, Lewer P, Müller C, Wagner J and Gombert A 2006 *Thin Solid Films* **511–512** 628
[7] Tvingstedt K, Dal Zilio S, Inganäs O and Tormen M 2008 *Opt. Express* **16** 21608
[8] Su M S, Kuo C Y, Yuan M C, Jeng U S, Su C J and Wei K H 2011 *Adv. Mater.* **23** 3315
[9] Yang J, Zhu R, Hong Z, He Y, Kumar A, Li Y and Yang Y 2011 *Adv. Mater.* **23** 3465
[10] Tvingstedt K, Tang Z and Inganäs O 2012 *Appl. Phys. Lett.* **101** 163902
[11] He Z, Zhong C, Huang X, Wong W-Y, Wu H, Chen L, Su S and Cao Y 2011 *Adv. Mater.* **23** 4636
[12] Dou L, You J B, Yang J, Chen C C, He Y J, Murase S, Moriarty T, Emery K, Li G and Yang Y 2012 *Nature Photon.* **6** 180
[13] Scharber M C, Mühlbacher D, Koppe M, Denk P, Waldauf C, Heeger A J and Brabec C J 2006 *Adv. Mater.* **18** 789
[14] Dennler G, Scharber M C, Ameri T, Denk P, Forberich K, Waldauf C and Brabec C J 2008 *Adv. Mater.* **20** 579
[15] Tvingstedt K, Andersson V, Zhang F L and Inganäs O 2007 *Appl. Phys. Lett.* **91** 123514
[16] Zhou Y H, Zhang F L, Tvingstedt K, Tian W J and Inganäs O 2008 *Appl. Phys. Lett.* **93** 033302
[17] Zhen H Y, Li K, Huang Z Y, Tang Z, Wu R M, Li G L, Liu X and Zhang F L 2012 *Appl. Phys. Lett.* **100** 213901
[18] Wang E G, Hou L T, Wang Z Q, Hellström S, Zhang F L, Inganäs O and Andersson M R 2010 *Adv. Mater.* **22** 5240
[19] Pandey A K, Nunzi J M, Ratier B and Moliton A 2008 *Phys. Lett.* A **372** 1333